Materials Science and Engineering B 177 (2012) 471–475

Contents lists available at SciVerse ScienceDirect

Materials Science and Engineering B

journal homepage: www.elsevier.com/locate/mseb

Magnetism and electrode dependant resistive switching in Ca-doped ceramic bismuth ferrite

D. Rubi[a,b,c,*], F.G. Marlasca[a], M. Reinoso[a,b], P. Bonville[d], P. Levy[a,b]

[a] GIA and INN, CAC-CNEA, 1650, San Martín, Argentina
[b] Consejo Nacional de Investigaciones Científicas y Técnicas, Buenos Aires, Argentina
[c] ECyT, Universidad Nacional de San Martín, San Martín, Buenos Aires, Argentina
[d] CEA Saclay, IRAMIS, SPEC (CNRS URA 2464), F-91191 Gif sur Yvette, France

ARTICLE INFO

Article history:
Received 20 September 2011
Received in revised form 9 January 2012
Accepted 19 February 2012
Available online 3 March 2012

Keywords:
$BiFeO_3$
Multiferroics
Resistive switching
RRAM

ABSTRACT

Here we report on the preparation and structural, magnetic and electrical characterization of $BiFeO_3$ and $Bi_{0.9}Ca_{0.1}FeO_3$ ceramic multiferroic samples. We suggest that Ca-doping creates oxygen vacancies and destabilizes the $BiFeO_3$ spiral magnetic structure. We also study resistive switching effects in $Bi_{0.9}Ca_{0.1}FeO_3$ with metallic electrodes, finding that the appearance of the effect is dependant on the fabrication procedure of the metallic electrode. On the basis of these observations, we critically revise some assumptions in currently available models of resistive switching of complex oxides.

1. Introduction

Bismuth ferrite ($BiFeO_3$) is a room temperature multiferroic material [1,2]; it is ferroelectric with a Curie temperature of around 1140 K, and antiferromagnetic with a Neel temperature of around 640 K. These properties, together with the possible coupling between magnetic and ferroelectric properties (through the so-called magnetoelectric effect), turn this material into a strong candidate for the development of novel storage and sensor devices. The $BiFeO_3$ antiferromagnetic structure is G-type and non-collinear, showing a cycloidal spiral spin arrangement in which the Fe^{3+} magnetic moments rotate in a plane with an incommensurate period $\lambda \sim 62$ nm [3]. Fe^{3+} magnetic moments are canted, resulting in a weak local magnetization that averages to zero over a period of the incommensurate modulated spin structure.

Resisitive switching (RS) is defined as the variation of the resistance of a material under the application of pulsed electrical stimulus (either voltage or current) [4,5]. This effect is usually reversible and non-volatile and has emerged ubiquitously in a great variety of simple and complex oxides. From technological point of view, interest arises from the possibility of taking advantage of the RS effect to fabricate novel Resistive Random Access Memories (RRAM). These memories were proposed to be a strong candidate to replace existent silicon based devices, such as flash memories. In the case of binary oxides, the RS effect is believed to arise from the electrical field induced creation/destruction of conducting filaments, connecting the electrodes through the insulating media [4]. On the contrary, in complex oxides, the effect is interface-related, that is, it takes place at the interface between the metal electrode and the oxide, playing a key role the presence of oxygen vacancies (which can be moved by the action of the electrical field during pulsing) that modulate the interface resistance [4]. $BiFeO_3$ has been shown to display resistive switching properties [6–11], enlarging the functionalities of the material and making it even more attractive from a technological point of view. Ramesh's group [6] found an electrical modulation associated to the migration of oxygen vacancies in Ca-doped $BiFeO_3$ thin films, resulting in hysteretic *I–V* curves that reflect a RS behavior, while Yin et al. [7] and Chen et al. [8] also found RS effects in thin films of the pristine (undoped) compound. Very recently, Qu et al. [9] reported non-volatile RS in $BiFeO_3$/Nb-$SrTiO_3$ heterojunctions, together with a substantial white-light photovoltaic effect, while Li et al. reported RS in La- and Ce-doped bismuth ferrite thin films [10,11].

In the present work, we synthesize and characterize $BiFeO_3$ and $Bi_{0.9}Ca_{0.1}FeO_3$ ceramic samples. We show by means of Mössbauer spectroscopy that Fe remains in a 3+ valence state upon Ca-doping. We also show that Ca-doping destabilize the $BiFeO_3$ spiral magnetic structure. Finally, we disclose a correlation between the appearance of RS in metal/$Bi_{0.9}Ca_{0.1}FeO_3$ system and the metallic electrodes fabrication procedure. We suggest that the usual rationalization of the resistive switching effect in complex oxides, involving the movement of oxygen vacancies close to the metal–oxide interface

* Corresponding author. Tel.: +54 11 67727059; fax: +54 11 67727121.
E-mail address: rubi@tandar.cnea.gov.ar (D. Rubi).

0921-5107/$ – see front matter © 2012 Elsevier B.V. All rights reserved.
doi:10.1016/j.mseb.2012.02.022

[12], seems to be too simple in this case, so a more complex scenario involving different chemical states of the metal constituting the electrode should be proposed.

2. Experimental

$BiFeO_3$ (BFO) and $Bi_{0.9}Ca_{0.1}FeO_3$ (BCFO) polycrystalline samples were prepared by means of standard solid state reactions. High purity (≥99.9%) Bi_2O_3 (Sigma–Aldrich), Fe_2O_3 (Sigma–Aldrich) and $CaCO_3$ (Normapur) oxides were weighted and mixed in appropriate ratios and fired in air for 15 h at 830 °C. We point out that both the firing temperature and time were adjusted to minimize the appearance of impurities. The composition and structure of the obtained powders were checked by means of X-ray diffraction (XRD) using a "D8 Advance" Bruker diffractometer with $Cu_{k\alpha}$ radiation ($\lambda = 1.5418$ Å). Afterwards, the powders were pressed and sintered overnight at 830 °C (BFO) and 860 °C (BCFO), respectively, leading to well sintered pellets suitable for electrical measurements. Mössbauer measurements have been carried out in the BCFO sample in order to investigate the state of Fe ions. The material was enriched with 30% of the ^{57}Fe isotope to allow for a good signal to noise ratio in a reasonable counting time. Mössbauer spectra were recorded at room temperature by using a constant acceleration drive spectrometer and a commercial ^{57}Co:Rh gamma ray source. The magnetization as a function of the applied field H was measured at 250 K under fields of up to 14 T by using an automated vibrating sample magnetometer (Cryogenic Ltd.). In order to perform electrical characterization, we prepared hand-painted silver electrodes (~1 mm^2) from commercial silver paste (CDS L-200). The electrodes were dried at room temperature for several hours before electrical measurements were performed. We also prepared 50 nm thick Ag, Al and Ti electrodes (arrays of 5 × 5 electrodes with a ~1 mm^2 surface) by e-beam evaporation at room temperature. Deposition was made through a home made shadow mask of aluminum foil. Electrical measurements were performed in a two terminals configuration with a Parameter Analizer Keithley 4200 and a Keithley 2400 source meter, both hooked to a Karl Suss probe station. Electrical measurements above room temperature (90 °C) were performed by placing the sample on top of a hot plate. Room temperature Raman spectra were recorded on a LabRAM HR Raman system (Horiba Jobin Yvon), equipped with two monochromator gratings and a charge coupled device detector (CCD). The Ar laser line at 514.5 nm was used as excitation source and it was filtered to give a laser fluence c.a. 1 W/mm^2 on the sample.

3. Results and discussion

Fig. 1 shows the XRD patterns corresponding to BFO and BCFO samples. The samples were single phase with the exception of a small amount of $Bi_{25}FeO_{40}$ impurity in the BFO sample (peaks marked with * in the inset (a) of Fig. 1). The presence of this impurity is suppressed in the case of the BCFO sample, indicating that Ca-doping eases the formation of the perovskite structure. The fact that we did not detect the presence of Bi-poor $Bi_2Fe_4O_9$ phase indicates that a significant Bi-loss did not take place during the synthesis of our samples [2]. For the BFO case, the XRD reflections were indexed in the well known rhombohedral structure (space group *R3c*, ICDD card 86-1518) with cell parameters $a = 5.577(3)$ Å and $c = 13.865(3)$ Å. The inset (b) of Fig. 1 shows a blow up of the XRD patterns of both BFO and BCFO samples. The inset shows that the single BFO peak located around 22.4° splits into two peaks in the BCFO spectrum, indicating a doping induced structural transition to a structure with a lower symmetry (triclinic with space group *P1*, according to Ref. [13]).

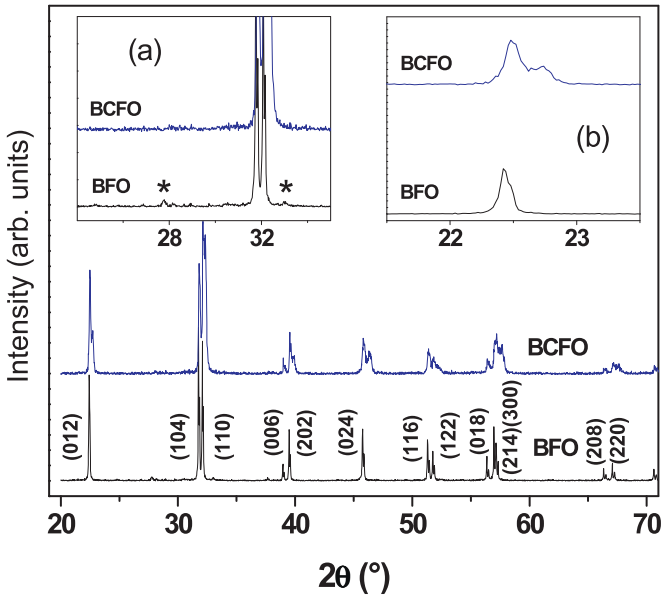

Fig. 1. (Main panel) XRD patterns corresponding to $BiFeO_3$ and $Bi_{0.9}Ca_{0.1}FeO_3$ samples, respectively. (Inset (a)) Blow up of the patterns showing the presence in the $BiFeO_3$ pattern of peaks, marked with *, corresponding to $Bi_{25}FeO_{40}$ impurity. (Inset (b)) Blow up of the patterns showing the splitting of the 22.4° $Bi_{0.9}Ca_{0.1}FeO_3$ peak, reflecting the transition to a structure with lower symmetry.

Fig. 2 shows the room temperature Mössbauer spectrum of a BCFO sample. The spectrum is composed of six symmetrical absorption lines characteristic of Fe^{3+} in a magnetic environment. The measured values for the hyperfine and the isomer shift were 49.5 T and 0.39 mm/s, respectively, typical for a Fe magnetic moment of $5\mu_B$. No traces of Fe^{4+} were found, suggesting that the substitution of trivalent Bi by divalent Ca does not modify the Fe valence but creates oxygen vacancies. Fig. 3(a) and (b) displays the evolution of the magnetization as a function of the applied magnetic field at 250 K for BFO and BCFO samples. Fig. 2(a) shows that the BFO magnetization increases linearly for low and intermediate fields, as expected for an antiferromagnetic spin structure. However, at a field $H \sim 9.5$ T the magnetization departs from linear behavior and for fields >9.5 T is clearly non-linear. This deviation from linearity is associated to a crossover from the spiral magnetic structure to a collinear

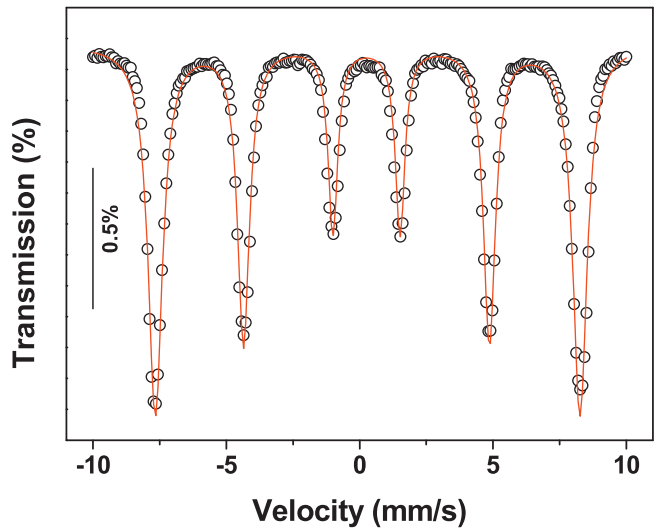

Fig. 2. Room temperature Mössbauer spectrum corresponding to the $Bi_{0.9}Ca_{0.1}FeO_3$ sample. Open symbols correspond to experimental values and the full line corresponds to the theoretical fitting of the spectrum.

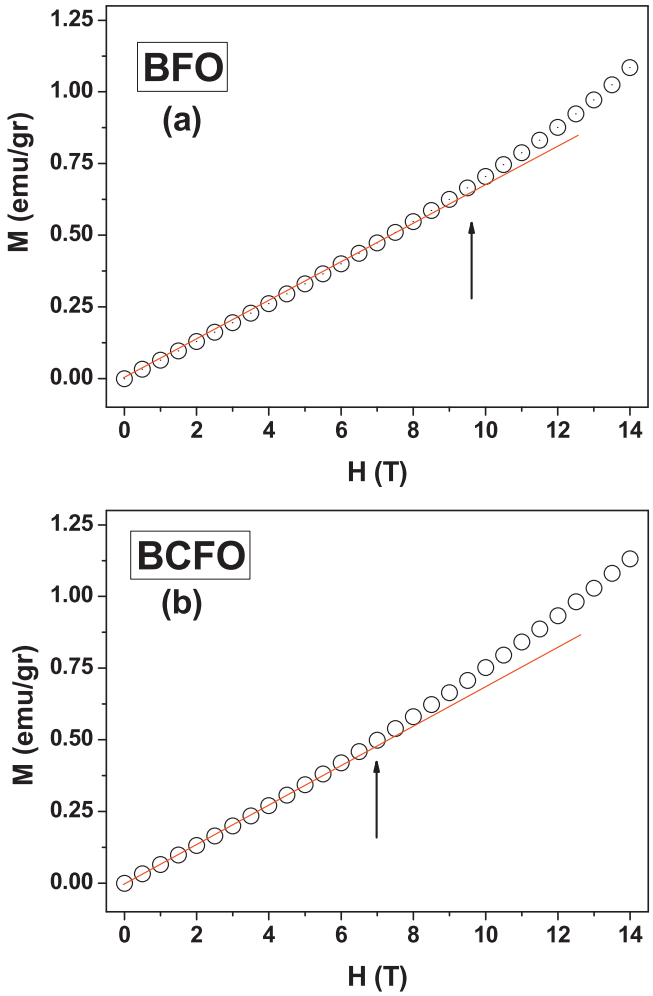

Fig. 3. (a and b) Magnetization as a function of the magnetic field at 250 K for $BiFeO_3$ and $Bi_{0.9}Ca_{0.1}FeO_3$ samples, respectively. The arrows indicate the departure of the magnetization from a linear behavior.

structure [14]. The magnetic behavior of the BCFO sample is qualitatively similar to the BFO sample, with the only difference that the threshold field for deviation from the linear behavior decreases to $H \sim 7$ T. This shows that Ca-doping reduces the transition field from the spatially modulated to the collinear magnetic state, as was also found for other dopants such as lanthanum [14]. We stress that the modification of the magnetic properties between BFO and BCFO is probably a consequence of structural changes upon Ca-doping, which modify the magnetic exchange among Fe ions.

We will discuss now the electrical properties. We should mention that pristine BFO sample was too resistive (two point resistances higher than 1 GΩ) to be measured with our experimental setup, so we will focus now on the BCFO sample, which showed lower (and measurable) resistances. First, we contacted the BCFO sample with hand painted commercial silver paste and we measured *I–V* curves with a Parameter Analizer Keithley 4200, which can provide voltages up to 20 V. Fig. 4(a) shows a typical room temperature *I–V* curve, being evident a non-linear behavior which reflects the non-ohmic character of the Ag/BCFO junction. Interestingly, no hysteresis is found in the *I–V* curve, reflecting the absence of resistive switching for this range (0–20 V) of electrical stimulus. We therefore pulsed the sample with the Keithley 2400 source meter, which can provide higher voltages (up to 200 V). Pulses with a time width around 1 ms were applied and the two terminals resistance was measured afterwards by applying a voltage bias of 3 V. Fig. 4(b) shows the evolution of the BCFO resistance as a function

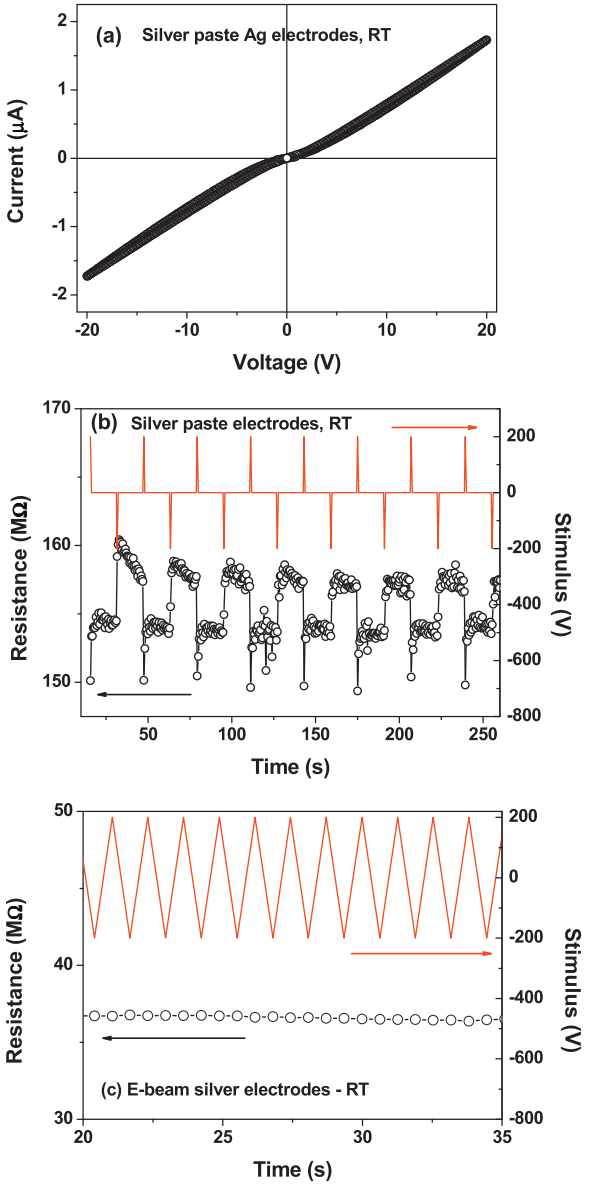

Fig. 4. (a) Room temperature intensity–voltage curve for the $Bi_{0.9}Ca_{0.1}FeO_3$ sample with hand painted silver electrodes, with applied voltages up to 20 V; (b) room temperature resistance as a function of time corresponding to $Bi_{0.9}Ca_{0.1}FeO_3$ with silver paste electrodes, pulsed with ±200 V; (c) room temperature resistance as a function of time for the $Bi_{0.9}Ca_{0.1}FeO_3$ sample with electron beam evaporated electrodes, pulsed with ±200 V.

of time upon pulsing with ±200 V. A bipolar resistive switching is evidenced, as the resistance reaches a maximum of ∼160 MΩ after the application of −200 V pulses, and a minimum of ∼153 MΩ following the application of +200 V pulses. We should mention that the RS was found to be forming free, that is, it shows up immediately after pulsing. We repeated the experiment at 90 °C (not shown here), finding that the RS effect nearly vanishes at higher temperatures, suggesting that diffusive processes, which are enhanced with the temperature, can counter back the resistance changes induced by the electrical field. We notice that the standard interpretation of the bipolar resistive switching effect in complex oxides such as BCFO is in terms of the electrical pulse induced migration of oxygen vacancies, which modify their concentration profile close to the metal–insulator junction [12] and change the resistance of the interface. Within this framework, a negative voltage applied to an Ag electrode induces the migration of positively charged oxygen

vacancies through the oxide to the metal–oxide interface. These vacancies accumulate close to the interface, resulting in a decrease of the Schottky potential barrier [4] and in a low resistance state. The application of an opposite voltage induces the movement of oxygen vacancies from the interface to the oxide bulk, increasing the Schottky potential barrier and resulting in a high resistance state. We should also mention that two terminals measurements involve electrical transport through two metal–oxide interfaces placed in opposition, that is, when one interface switches from low resistance to high resistance the other interface switches inversely, in which is called a "complementary effect" [15]. In consequence, what one can measure in a two terminals configuration is an unbalance of the two interfaces, which should be favored by the existence of any kind of asymmetry between both of them. In our case, this asymmetry comes from slight differences in the geometry of the electrodes.

In order to get further evidence of the RS effect and the validity of the model described above, we systematically changed the metal–BCFO interface by preparing samples with different electrodes (Ag, Al, Ti) deposited at room temperature by electron-beam evaporation. As the deposition was performed through a home made shadow mask, the area of the electrodes (nominally 1 mm^2) presents some dispersion (±15%, similar to the case of hand-painted silver paste electrodes). We measured on several pairs of electrodes along the sample, in particular those displaying more evident differences in area (most asymmetric). Interestingly, we have not been able to observe resistive switching in any of these systems, as shown in Fig. 4(c) for the case of Ag/BCFO system pulsed with ±200 V, where it is evident that the resistance does not significantly change upon pulsing. Remarkably, in the case of Ag electrodes, the observation of the RS effect seems to be dependant on the fabrication procedure of the electrode: we measured RS for hand-painted silver paste electrodes and we did not observe the effect for e-beam evaporated electrodes. This dependence of the RS with the electrode preparation technique has been previously observed in other systems but its origin remains elusive. For example, as raised by Dong et al. [16], Shang et al. [17,18] and Fujimoto et al. [19] found hysteretic *I–V* curves and RS in $Ag/(La,Pr)_{0.7}Ca_{0.3}MnO_3/Pt$ systems, where the Ag electrode was painted with silver paste, while Liao et al. [20] found no resistive switching in $Ag/Pr_{0.7}Ca_{0.3}MnO_3/Pt$, where the Ag electrode was prepared by magnetron sputtering. This variety of results suggests that RS behavior depends not only on the nature of the metal/oxide system and on modifications of the oxygen vacancies profiles, but also on the existence of some sort of chemical reaction at the interface. A possible scenario is related to the reaction of the metal to form an oxide (AgO_x in the case of silver electrodes). For instance, Dong et al. [16] reported that $Ag/AgO_x/WO_{3-x}/Pt$ displays RS behavior (where the silver oxide was deliberately fabricated by depositing silver in an oxygen reactive atmosphere) while $Ag/WO_{3-x}/Pt$ does not. They conclude that an electrochemical redox reaction occurs at the AgO_x layer: silver and oxygen ions are driven to the two opposite sides of the AgO_x layer by the electrical field and then decomposed into metallic silver and O atoms. The metallic silver damages the AgO_x/WO_{3-x} interface barrier, resulting in the decrease of the device resistance. Under negative bias, the metallic silver is reoxidized and the device returns to the high resistance state. In our case, a similar scenario could be present and the appearance of RS could be also arguably related to the existence of AgO_x oxide at the Ag/BCFO interface and an electrochemical reaction as previously described. In the case of silver paste hand painted electrodes, the oxidation of silver could take place due to the existence of available oxygen in the solvent/epoxy of the paste. On the contrary, electron beam deposition of silver is done in vacuum where no oxygen is available to oxidise the silver (electrodes are well bonded to the substrate and this precludes the possibility of oxidation of the interface upon exposure to air). Moreover, the oxygen deficient character of BCFO (as inferred from Mössbauer measurements) may hamper the possibility of oxygen transfer from BCFO to silver and a subsequent oxidation. The room temperature Raman spectra of Fig. 5, recorded for both types of electrodes after electrical measurements under the same conditions, show the presence of several bands for silver paste electrodes while no bands can be observed for e-beam electrodes. This indicates different chemical composition for both types of electrodes. The most prominent bands found in the former case (which have been observed even in electrodes painted several months before Raman measurements) are associated with C–O, C–C stretching or C–H bending modes (near 1500 cm^{-1}), C–H stretching modes (near 3000 cm^{-1}) and C–C–C bending modes (near 650 cm^{-1}) suggesting the presence of remains of organic solvent [21,22]. The presence of these oxygen rich solvent traces could be at the origin of the electrochemical reaction with metallic silver, leading to the formation of silver oxide at the metal–oxide interface. In consequence, the system Ag + AgO_x/BCFO may display RS while the system Ag/BCFO may not. The latter scenario (that is, the absence of metal oxidation) could apply to the case of the other electrodes (Al, Ti) deposited by electron-beam evaporation, which also did not display RS. This indicates that, at least for metal/BCFO systems, the scenario previously described involving electrical-field induced movement of oxygen vacancies – that modulate the Schottky potential barrier – is too naïve and a more complex scenario involving different chemical states of the metal constituting the electrode should be proposed.

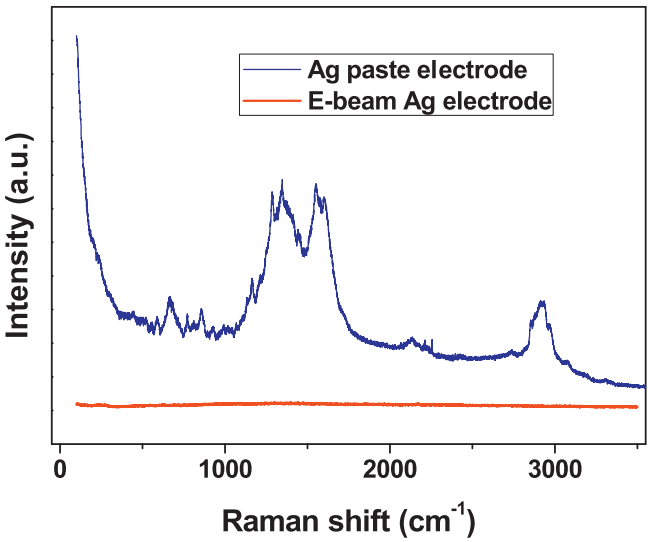

Fig. 5. Room temperature Raman spectra corresponding to both hand-painted paste and e-beam silver electrodes. The silver paste spectrum was shifted for sake of clarity.

4. Conclusions

In summary, we successfully synthesized BFO and BCFO ceramic samples and characterized their structural, magnetic and electrical properties. The creation of oxygen vacancies upon Ca-doping was inferred from Mössbauer spectroscopy. Magnetic measurements suggest that Ca-doping also destabilizes the pristine BFO spiral magnetic structure. Regarding electrical transport properties, we have shown that resistive switching effect in metal/BCFO systems is dependant on the fabrication procedure of the metallic electrode: we found RS for silver paste hand painted electrodes while no RS was found for electron-beam deposited electrodes. We attribute this difference to silver oxide formation in the former, which facilitates the appearance of RS via an electrochemical reaction. Our data

suggest that the RS mechanism is likely to be more complex that the one usually proposed involving changes in the oxygen vacancies profile close to the metal/oxide interface; in consequence, a word of caution should be put on the interpretation of resistive switching effects in metal/complex oxide systems.

Acknowledgements

We thank financial support from CONICET (projects MeMO-PIP 2008-11220080100047 and CONICET-Dupont), Fundación Balseiro and Univ. Nacional de San Martín.

References

[1] G. Catalán, J.F. Scott, Adv. Mater. 21 (2009) 2463.
[2] D. Lebeugle, D. Colson, A. Forget, M. Viret, P. Bonville, J.F. Marucco, S. Fusil, Phys. Rev. B 76 (2007) 024116.
[3] I. Sosnowska, T. Peterlin-Neumaier, E. Steichele, J. Phys. C 15 (1982) 4835.
[4] A. Sawa, Mater. Today 11 (2008) 28.
[5] R. Waser, R. Dittmann, G. Staikov, K. Szot, Adv. Mater. 21 (2009) 2632–2663.
[6] C.-H. Yang, J. Seidel, S.Y. Kim, P.B. Rossen, P. Yu, M. Gajek, Y.H. Chu, L.W. Martin, M.B. Holcomb, Q. He, P. Maksymovych, N. Balke, S.V. Kalinin, A.P. Baddorf, S.R. Basu, M.L. Scullin, R. Ramesh, Nat. Mater. 8 (2009) 485.
[7] K. Yin, M. Li, Y. Liu, C. He, F. Zhuge, B. Chen, W. Lu, X. Pan, R.W. Li, Appl. Phys. Lett. 97 (2010) 042101.
[8] X. Chen, G. Wu, H. Zhang, N. Qin, T. Wang, F. Wang, W. Shi, D. Bao, Appl. Phys. A 100 (2010) 987.
[9] T.L. Qu, Y.G. Zhao, D. Xie, J.P. Shi, Q.P. Chen, T.L. Ren, Appl. Phys. Lett. 98 (2011) 173507.
[10] M. Li, F. Zhuge, X. Zhu, K. Yin, J. Wang, Y. Liu, C. He, B. Chen, R.W. Li, Nanotechnology 21 (2010) 425202.
[11] X. Zhu, F. Zhuge, M. Li, K. Yin, Y. Liu, Z. Zuo, B. Chen, R.W. Li, J. Phys. D: Appl. Phys. 44 (2011) 415104.
[12] M.J. Rozenberg, M.J. Sánchez, R. Weht, C. Acha, F. Gomez-Marlasca, P. Levy, Phys. Rev. B 81 (2010) 115101.
[13] D. Kothari, V.R. Reddy, A. Gupta, V. Sathe, A. Banerjee, S.M. Gupta, A.M. Awashti, Appl. Phys. Lett. 91 (2007) 202505.
[14] G. Le Bras, D. Colson, A. Forget, N. Genand-Riondet, R. Tourbot, P. Bonville, Phys. Rev. B 80 (2009) 134417.
[15] M. Quintero, P. Levy, A.G. Leyva, M.J. Rozenberg, Phys. Rev. Lett. 98 (2007) 116601.
[16] C.Y. Dong, D.S. Shang, L. Shi, J.R. Sun, B.G. Shen, F. Zhuge, R.W. Li, W. Chen, Appl. Phys. Lett. 98 (2011) 072107.
[17] D.S. Shang, Q. Wang, L.D. Chen, R. Dong, X.M. Li, W.Q. Zhang, Phys. Rev. B 73 (2006) 245427.
[18] D.S. Shang, L.D. Chen, Q. Wang, Z.H. Wu, W.Q. Zhang, X.M. Li, J. Mater. Res. 23 (2008) 302.
[19] M. Fujimoto, H. Koyama, Y. Nishi, T. Suzuki, Appl. Phys. Lett. 91 (2007) 223504.
[20] Z.L. Liao, Z.Z. Wang, Y. Meng, Z.Y. Liu, P. Gao, J.L. Gang, H.W. Zhao, X.J. Liang, X.D. Bai, D.M. Chen, Appl. Phys. Lett. 94 (2009) 253503.
[21] M.J. Pelletier, Analytical Applications of Raman Spectroscopy, Wiley-Blackwell, UK, 1999.
[22] J.G. Grasselli, B.J. Bulkin, Analytical Raman Spectroscopy, Wiley Interscience, New York, 1991.